ARCHIVES of FOUNDRY ENGINEERING

ISSN (1897-3310)
Volume 11
Issue 4/2011

149 – 156

28/4

Published quarterly as the organ of the Foundry Commission of the Polish Academy of Sciences

Control of the structural parameters in the (Zn) – Zn16Ti single crystal growth

W. Wołczyński[a]*, G. Boczkal[b], P. Musielak[b], G. Sibiga[b], B. Mikułowski[b]
[a] Institute of Metallurgy and Materials Science, Reymonta 25, 30-059 Kraków, Poland
[b] AGH – University of Science and Technology, Mickiewicza 30, 30-059 Kraków, Poland
*Corresponding author. E-mail address: nmwolczy@imim-pan.krakow.pl

Received 27.06.2011 accepted in revised form 27.07.2011

Abstract

The (Zn) - single crystal was obtained by means of the Bridgman system. Several growth rates were applied during the experiment. The graphite crucible was used in order to perform the solidification process. The unidirectional solidification occurred with the presence of the moving temperature field. The thermal gradient was positive so that the constrained growth of the single crystal was ensured. The (Zn) single crystal was doped with small addition of titanium and copper. The titanium formed an intermetallic compound Zn16-Ti. The copper was solved in the solid solution (Zn). The precipitates of (Zn) and Zn16-Ti formed a stripes localized cyclically along the single crystal length. The intermetallic compound Zn16-Ti strengthened the (Zn) single crystal. The structural transitions were observed in the stripes with the increasing solidification rate. Within the first range of the solidification rates ($0 \div v_1$) the irregular L-shape rod-like intermetallic compound was revealed. At the v_1 - threshold growth rate branches disappear continuously till the growth rate equal to v_1'. At the same range of growth rates the regular lamellar eutectic structure (Zn) – Zn16-Ti appeared continuously and it existed exclusively till the second threshold growth rate equal to v_2. Above the second threshold growth rate the regular rod-like eutectic structure was formed, only. The general theory for the stationary eutectic solidification was developed. According to this theory the eutectic structure localized within the stripes is formed under stationary state. Therefore, the criterion of the minimum entropy production defines well the stationary solidification. The entropy production was calculated for the regular rod-like eutectic structure formation and for the regular lamellar eutectic structure formation. It was postulated that the observed structure are subjected to the competition. That is why the structural transition were observed at the revealed threshold growth rates. Moreover, it was postulated that this structure is winner in the competition which manifests a lower minimum entropy production within a studied range of growth rates. Exceptionally, the phenomenon of branching was formed under the marginal stability. Therefore, the spacing of the regular structure selected by the criterion of minimum entropy production depends on the growth rate only. In the case of the irregular eutectic structure the average spacing depends on both growth rate and thermal gradient. The irregular eutectic structure localized within the stripes contains some areas with regular rods and some areas with maximum destabilization of solid / liquid interface of the (Zn) - non-faceted phase. The length of the destabilized non-faceted phase is treated as equal to the wavelength of the perturbation which appears at the solid / liquid interface of the non-faceted phase, (Zn). In spite of the interface destabilization the selection of a given structure depends on the localization of the minimum entropy production, only.

Keywords: Hexagonal single crystal, Strengthening by intermetallic precipitates, Minimum entropy production, Structural transitions, Principle of the lower minimum entropy production, Single crystal with stripes

1. Introduction

Many eutectic systems exhibit either a lamellar or rod-like structure depending on solidification conditions, Elliott, [1]. Especially, growth rate plays a crucial role in the lamella / rod transformation. Some impurities also involve the transition, Steen and Hellawell, [2]. The impurities change the specific surface free energies and finally modify a mechanical equilibrium at the triple point of the solid/liquid interface. According to the current model assumptions, the mechanical equilibrium varies with solidification conditions (growth rate) and no effect of impurities is observed. A given orientation of the crystal depends on an imposed growth rate. Some changes of the orientation from an initial state into a final one give also an effect on the lamella / rod transition, [3].

The theory developed by Jackson and Hunt, [4] has tried to predict the threshold rate at which transformation should occur. It yields an inequality according to which:

$$\left(a_{\alpha}^{L}/m_{\alpha}+a_{\beta}^{L}/\xi m_{\beta}\right)/\left(a_{\alpha}^{R}/m_{\alpha}+a_{\beta}^{R}/\xi m_{\beta}\right)> \left(4E/P\right)\left(1/\left(1+\xi\right)^{1.5}\right) \quad (1)$$

The discerning analysis shows that the above inequality can predict whether an eutectic alloy manifests lamellar or rod-like structure, only. E, P and a_j^L, a_j^R - parameters delivered in the J-H theory, [4], $j=\alpha,\beta$, $\xi = S_{\beta}/S_{\alpha}$, and m_j - slope of the liquidus lines, [K/mole fr.]; respectively, $j=\alpha,\beta$.

Thus, the inequality characterizes a given phase diagram. Therefore, Eq. (1) cannot be applied to describe the structural transformations which occur in the same eutectic alloy in function of the varying growth rate.

It is evident that the Eq. (1) is completely misleading in the case of some predictions connected with structural transformation. Therefore, a new condition for transformation based on the calculation of the minimum entropy production will be applied in the current analysis. All the threshold growth rates will be determined for the (Zn)-$Zn_{16}Ti$ eutectic system by means of the current theorem. According to the current theorem this structure is the stable form which manifests the lower minimum entropy production within the adequate range of solidification rates.

2. Result of solidification experiments

In this study, the strengthening phenomenon is obtained for the hexagonal (Zn) - single crystal which contains regular layers of the Zn16-Ti precipitates.

According to the Zn-Ti phase diagram the solubility of Ti in the Zn is equal to 0.000546 [at.%] at the ambient temperature. Thus, the strengthening by a Ti - solubility can be neglected. However, the strengthening by the eutectic precipitates is possible and this phenomenon was studied experimentally, for different solute contents: I, II, III, Fig. 1.

Since the difference between melting point of the Zn and eutectic temperature is small it involves a possibility of the (Zn) - single crystal strengthening by the periodic precipitates of eutectic phase ((Zn) + Zn16-Ti).

The (Zn) eutectic phase is the same as the phase of the bulk material, Fig. 2. Therefore, it can be suggested that the Zn16-Ti eutectic phase is responsible for a strengthening, only. Really, the small addition of copper (0.1%) was solved in the (Zn) - solid solution. The copper does not form any intermetallic compound.

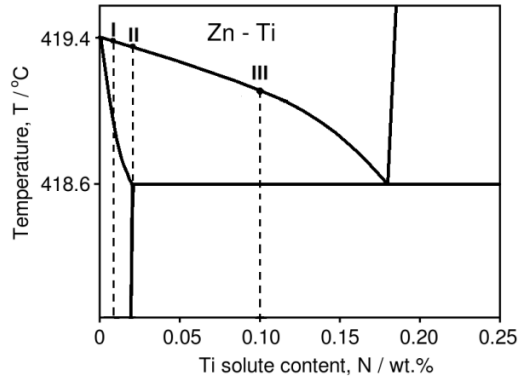

Fig. 1. Zn-Ti phase diagram which shows the localization of the eutectic point, $N_E = 0.18\,[wt\%Ti]$, [5]

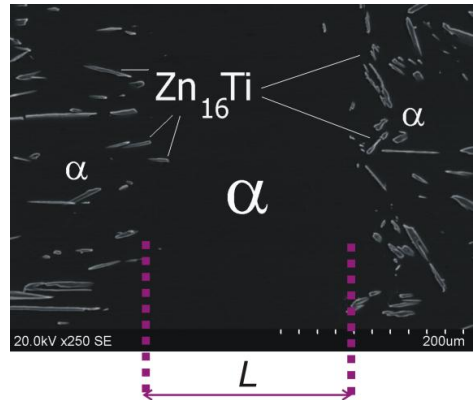

Fig. 2. Definition of the L - distance marked between two stripes or width of a bulk $(Zn)=\alpha$ crystal located between two stripes

The single crystals were obtained by the *Bridgman* method at the various growth rates. The single crystals had dimensions 6x6x150 [mm^3]. Several growth rates were applied: the smallest rate was equal to 1.8, and the highest was equal to 16 [mm/h]. All the crystal seeds were oriented by a diffraction method.

The obtained single crystal morphology depends on the growth rate applied in experiment, Fig. 3. Two threshold rates appeared in the single crystal growth. Below first threshold rate, L-shape structure (rod-like structure), Fig. 3a, with branches, Fig. 3b, was observed within the strengthening stripes. Above this threshold growth rate, the L-shape rods equipped with branches transformed into regular lamellar structure and finally the regular lamellar structure existed till the second threshold rate, Fig. 3c.

At the second threshold rate the regular lamellae transformed into rods, Fig. 3d, and rod-like structure appeared exclusively in the stripes above the second threshold growth rate, Fig. 3e.

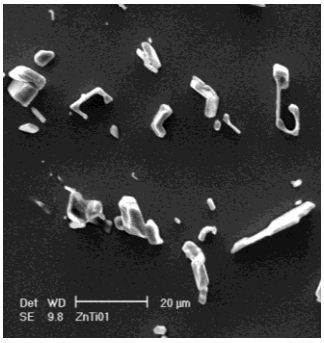

a)

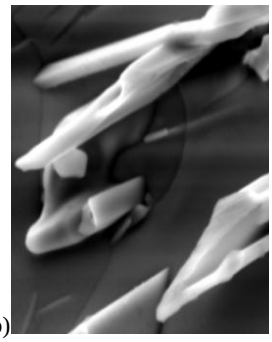
b)

Fig. 3a. Precipitation of the Zn16-Ti intermetallic compound of the L-shape structure obtained for the growth rates lower than v_1
Fig. 3b. Branching of the Zn16-Ti intermetallic compound for the L-shape structure when the growth rates are lower than v_1

The branches disappeared in the range of rates from v_1 till v_1'.

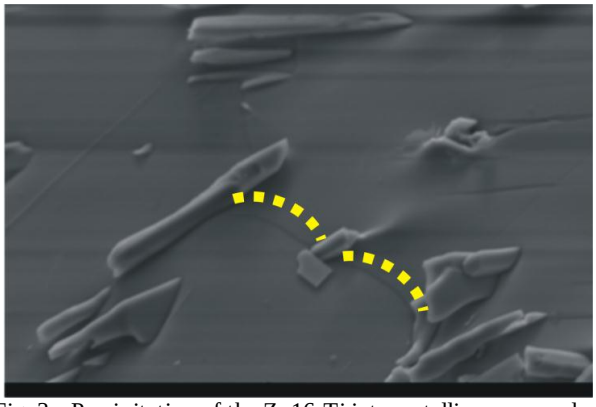

Fig. 3c. Precipitation of the Zn16-Ti intermetallic compound of the regular lamellar structure as obtained for the imposed growth rates situated upper v_1', and lower than v_2

Since the revealed solid / liquid interface is parabolic one and no interface destabilization is observed (between two lamellae) it is evident that the obtained structure is the regular structure.

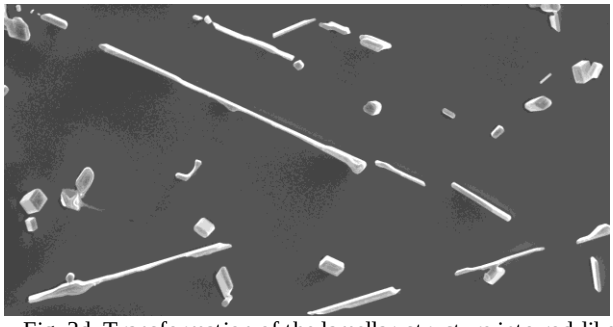

Fig. 3d. Transformation of the lamellar structure into rod-like structure at the threshold growth rate equal to v_2

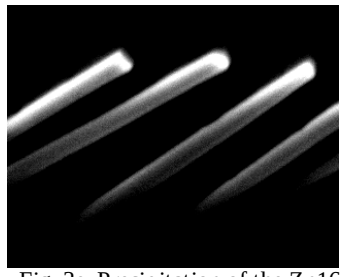

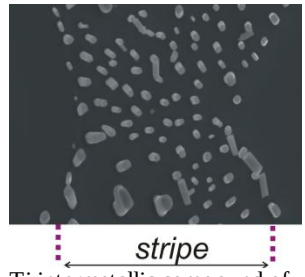

Fig. 3e. Precipitation of the Zn16-Ti intermetallic compound of the regular rods as obtained for the growth rates higher than v_2

According to the results of experiment a control of the stripe thickness and the inter-stripe spacing seems to be possible. It gives a possibility to optimize some properties of the final products made of the single crystal. Thus, a proper model which allows the control is necessary. It is suggested to apply the solute redistribution model which takes into account the phenomena of partitioning and back-diffusion, [6].

3. Model of solute redistribution

The Zn-Ti binary phase diagram gives a possibility of an easy control of the stripe thickness, Fig. 4.

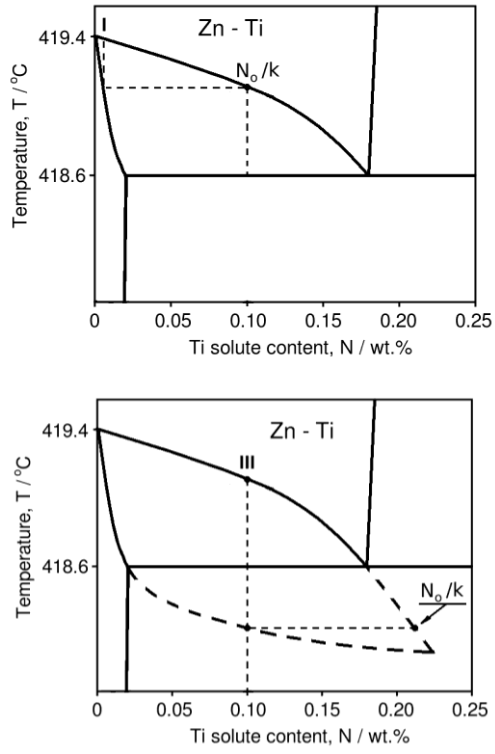

Fig. 4. The (Zn)-$Zn_{16}Ti$ pseudo-binary phase diagram which illustrates the so-called equilibrium solidification (full back-diffusion) for the Ti - nominal solute concentration being equal to: a/ I; I = N_0 = 0.01 [wt%] Ti), b/ III; III = N_0 = 0.1 [wt%] Ti

When solidification occurs near the equilibrium, the I – alloy does not give a possibility of the (Zn) single crystal strengthening, Fig. 4a. However, the stripes are stable form while applying an alloy of the III – nominal Ti – solute concentration, Fig. 4b.

Brody and Flemings, [7] have delivered a theory for solute microsegregation accompanied by a back-diffusion phenomenon which is defined by the back-diffusion parameter, α:

$$\alpha = D_S \, t_l \, B^{-2} \tag{2}$$

where D_S - diffusion coefficient into the solid, [m^2/s]; t_l - local solidification time, [s]; B - half the dendrite spacing, [m].

The B-F theory is not able, however, to describe the solute redistribution. Mass balance is not satisfied, and the α back-diffusion parameter tends towards infinity in the B-F theory, [7].

Therefore, an improved model, [6], based on the definition of α back-diffusion parameter, (2) was delivered. The model describes the solute redistribution after back-diffusion and can be used for calculating an amount of precipitates. The equation describing the solute redistribution after back-diffusion is:

$$N^B\left(x;X^0,\alpha\right)=\left[k+\beta^{ex}\left(x;X^0\right)\beta^{in}\left(X^0,\alpha\right)\right]N^L\left(x;\alpha\right) \tag{3}$$

k - partition ratio, x - growing crystal amount, [dimensionless];
$x = X^0$ - amount of the crystal at which solidification is stopped,
β^{ex} - coefficient of the redistribution extension, [dimensionless];
β^{in} - coefficient of the redistribution intensity, [dimensionless];
N^L - solute concentration in the liquid, [mole fraction]; (4).

$$N^L\left(x;\alpha\right)=N_0\left(1+\alpha\, k\, x-x\right)^{(k-1)/(1-\alpha k)} \tag{4}$$

which results from the differential equation for microsegregation accompanied by the back-diffusion, (5):

$$\left[1+\alpha\, k\, x-x\right]dN^L\left(x;\alpha\right)=\left(1-k\right)N^L\left(x;\alpha\right)dx \tag{5}$$

Both, β^{ex} - coefficient of the redistribution extension and β^{in} - coefficient of the redistribution intensity are defined in details, [6]. Their product $\beta\left(x;X^0,\alpha\right)=\beta^{ex}\left(x,X^0\right)\beta^{in}\left(X^0;\alpha\right)$ is equal to zero $\beta\left(x;X^0,0\right)=0$ for non-equilibrium solidification (when $\alpha=0$) and equals $\left(1-k\right)\left(1-x\right)$ for equilibrium solidification (when $\alpha=1$, with, $X^0=1$), $\beta\left(x;1,1\right)=\left(1-k\right)\left(1-x\right)$.

It can be assumed that the single crystal growth occurs so slowly that its growth is performed under condition close to the equilibrium, Fig. 4. The definition of the final amount of crystal just after solidification, x_K, dimensionless, is as follows:

$$x_K\left(\alpha,N_0\right)=\frac{1}{1-\alpha k}\left[1-\left(\frac{N_E}{N_0}\right)^p\right],\qquad p=\frac{1-\alpha k}{k-1} \tag{6}$$

Equation (6) is valid when $0\le\alpha\le\alpha_E\left(N_0\right)$. However, when $\alpha_E\left(N_0\right)<\alpha\le 1$, then $x_K\left(\alpha,N_0\right)=1$, with N_E - solute content in eutectic point, $\left(\alpha_E k\right)^{p'}=N_E/N_0$ and $p'=\left(k-1\right)/\left(1-\alpha_E\, k\right)$. Thus, the total amount of eutectic precipitates is given as:

$$i_K\left(\alpha,N_0\right)=1-x_K\left(\alpha,N_0\right) \tag{7}$$

4. Control of the precipitates amount

A specific morphology of the phase diagram, Fig. 4., involves a possibility of the easy control of the precipitates amount and the inter-stripe distance (defined in Fig. 2.). The current model for redistribution (2) – (7) was used to predict the precipitation mode of the multi-layers, (set of the stripes), Fig. 5. The stripes are composed of (Zn) - phase and intermetallic phase Zn16-Ti, Fig. 2, Fig. 3. The result of simulation are shown in Fig. 6.

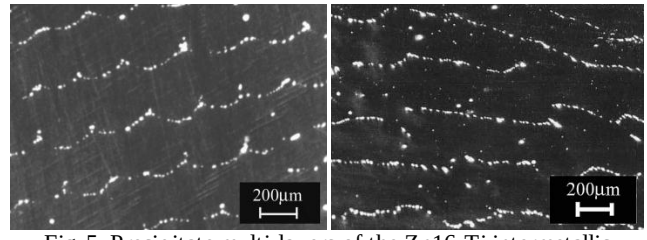

Fig. 5. Precipitate multi-layers of the Zn16-Ti intermetallic compound (bright areas) for the (Zn) - single crystal grown by the *Bridgman* system, $v=3\,[mm/h]$; a/ for $N_0=I=0.01\,[wt.\%Ti]$, b/ for $N_0=II=0.02\,[wt.\%Ti]$

An attempt to predict segregation / redistribution within a single crystal of the manganese – zinc ferrites obtained by the open *Bridgman* system has already been done, [8], [9]. However, in the case of the ferrites single crystal growth there were no precipitates.

In the case of the current study the *Bridgman* furnace has been working as a closed system and the control of strengthening could be done, to some extent, by an adequate choose of a nominal concentration of titanium in the alloy used for single crystal growth and by applying a proper growth rate, v, on which the $\alpha(v)$ - back-diffusion parameter, (2), depends.

The curves shown in Fig. 6., illustrate the result of the single crystal, (Zn), solidification by the *Bridgman* system twice:
a/ for the $N_0=II=0.02\,[wt.\%Ti]$,
b/ for the $N_0=III=0.1\,[wt.\%Ti]$.
Moreover, simulation was made for two different situations;
a/ with no back-diffusion, $\alpha=0$,
b/ with the proper value of the back-diffusion parameter, $\alpha\neq 0$.

According to obtained result of simulation it was confirmed that the control of the single crystal morphology is possible by:
a/ imposing different nominal solute concentration, N_0,
b/ adjustment of a proper value of the back-diffusion parameter.

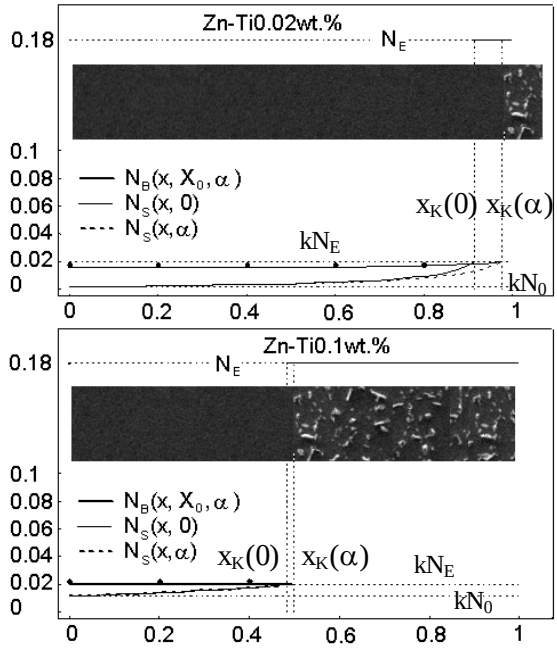

Fig. 6. Ti - solute redistribution versus the amount of the single crystal: a/ $N_0 = 0.02$, b/ $N_0 = 0.1$, [wt.%]; with $N_E = 0.18$, [wt.%], $k = 0.11$, [wt.%/wt.%], as defined in Fig. 1.; $N_B(x, X_0, \alpha)$ – solute redistribution after back-diffusion, [wt. fr.]; $N_S(x,0)$ – solute content at the s/l interface with no diffusion, [10], $N_S(x,\alpha)$ - solute content at the s/l interface with back-diffusion, [6], $\alpha = 0.31$, dimensionless, $X_0 = 1$, $x_K(0, N_0)$, $x_K(\alpha, N_0)$ are given by equation (6); results of simulation are superposed on the real morphology of the experimentally observed single crystal in which $x_K(\alpha)$ determines an amount of the bulk single crystal contained between two stripes, Fig. 2.; $1 - x_K(\alpha) = i_K(\alpha)$, (according to equation (7)), determines an amount of the precipitate, Fig. 3e''; the calculated Ti-solute redistribution fits points of Ti - solute content determined by the EDS measurement

5. Selection of single crystal morphology

Some successive observations of the (Zn) – single crystal growth allow to reveal two threshold growth rates at which structural transformations occur as mentioned in section 2. The following values of characteristic growth rates were stated:

$0 < v < v_1$ L-shape rods equipped with branches, Fig. 3a''.

$v_1 < v < v_1'$ L-shape rods with disappearing branches and regular lamellae, amount of which increases continuously,

$v_1' < v < v_2$ regular lamellae which are formed exclusively,

$v > v_2$ regular rods which exist exclusively within the range of crystal growth rates, v.

These growth rates have following experimental values:

$v_1 = $ 5 [mm/h]; $v_1' = $ 5.8 [mm/h]; $v_2 = $ 10 [mm/h].

It seems possible to predict theoretically why a given type of morphology appears within an observed range of growth rates.

Therefore, the entropy production was calculated for the formation of each of the observed structure: L-shape rods, lamellae and rods. The entropy production is given as an integral:

$$P = \int_V \sigma \, dV \tag{8}$$

where, V is the so-called „thermodynamic macroscopic point" inside of which all the essential fluxes are observed, Fig. 7, σ is the entropy production per unit time and per unit volume, and P is the entropy production per unit time (total entropy production).

$$\sigma = \sum_j X_j J^j = R \zeta C^{-1} (1 - C)^{-1} D \nabla^2 C \tag{9}$$

X - general thermodynamic force, J - general thermodynamic flux, j - number of fluxes, C - solute content, R - gas constant, ζ - thermodynamic factor, D - diffusion coefficient in the liquid.

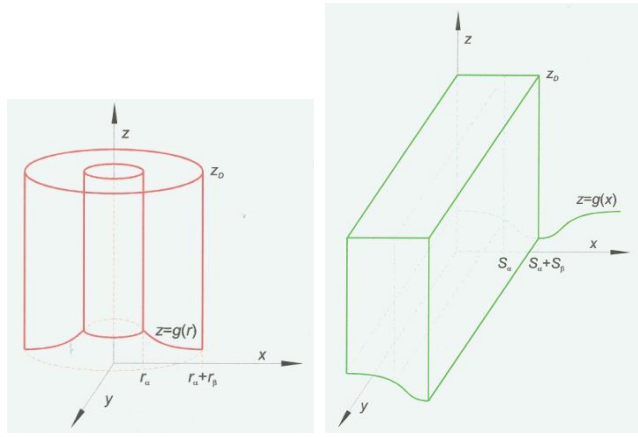

Fig. 7. Volume V used in the determination of the entropy production, a/ for the rod-like structure, r_α - rod radius, r_β - matrix thickness, $z = g(r)$ function describes the s/l interface shape, z_D - thickness of the diffusion zone; b/ for the lamellar structure, S_α - half the width of α - lamella, S_β - half the width of β - lamella, $z = g(x)$ - function describes the s/l interface shape

The entropy production per unit time is written as follows:
a/ for the regular rod-like structure formation (with no branches):

$$P_R = V_1 v \left(r_\alpha + r_\beta\right)^{-1} + V_2 v \left(r_\alpha + r_\beta\right)^{-2} + V_3 v^2 + V_4 v^2 \left(r_\alpha + r_\beta\right) + V_5 v^3 \left(r_\alpha + r_\beta\right)^2 \tag{10a}$$

b/ for the regular lamellar structure formation:

$$P_L = W_1 v\left(S_\alpha + S_\beta\right)^{-1} + W_2 v\left(S_\alpha + S_\beta\right)^{-2} + W_3 v^2 + W_4 v^2\left(S_\alpha + S_\beta\right) + W_5 v^3\left(S_\alpha + S_\beta\right)^2 \quad (10b)$$

where, V_i and W_i are the material constants, $i = 1,...,7$, [11].

Additionally, the rotation of the mechanical equilibrium situated at the triple point of the s/l interface was assumed, Fig. 8.

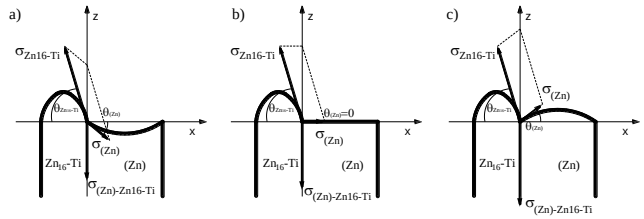

Fig. 8. Rotation of the mechanical equilibrium established by the parallelogram of the anisotropic specific surface free energies; s/l interface curvature changes with the crystallographic orientation rotation; $\sigma_{(Zn)} \equiv \sigma^L_{(Zn)}$, and $\sigma_{Zn16-Ti} \equiv \sigma^L_{Zn16-Ti}$ - specific surface free energies for (Zn) - phase and $Zn_{16}Ti$ - phase, respectively, $\sigma_{(Zn)-Zn16Ti}$ - inter-phase energy, θ_j - angles, $j = \alpha, \beta$

The proper values of the capillary parameters result from the rotation o of the mechanical equilibrium, as shown in Fig. 8. This model was confirmed experimentally since the curvature of the s/l interface was frozen while arresting the solidification.

Some changes of the specific surface free energy accompanied by the adequate changes of the inter-phase energy were analyzed.

The analysis allowed to show these capillary parameters varying with the growth rates, (rate of solidification), Fig. 9.

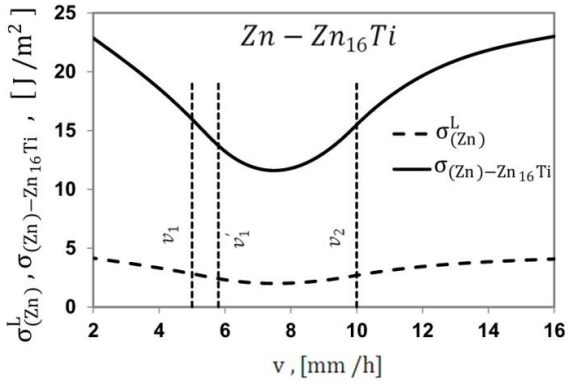

Fig. 9. Changes of specific surface free energy, $\sigma_{(Zn)} \equiv \sigma^L_{(Zn)}$, and inter-phase energy $\sigma_{(Zn)-Zn16Ti}$ for the investigated system as it results from the rotation of the mechanical equilibrium

The appearance of the observed structure is accompanied by a proper entropy production, as postulated. Since the considered solidification occurs under stationary state, [12], therefore the entropy production manifests its minimum, [13].

It is suggested that the entropy production calculated for a given structure formation within a proper range of growth rates, locates its minimum lower than the entropy production determined for a competitive structure.

Thus, for the range of growth rates, $0 \div v_1$, the minimum entropy production for the L-shape rods formation is situated lower than the minimum entropy production for the regular lamellae formation. Analogously, for the range of growth rates, $v_1 \div v_2$ the minimum entropy production for the regular lamellar structure formation should be situated lower than the minimum entropy production for the regular rod-like structure formation observed above the v_2 - threshold rate.

Finally, the entropy production was calculated according to equation (10) for analyzed types of stripes structure. The results of calculation are shown in Fig. 10.

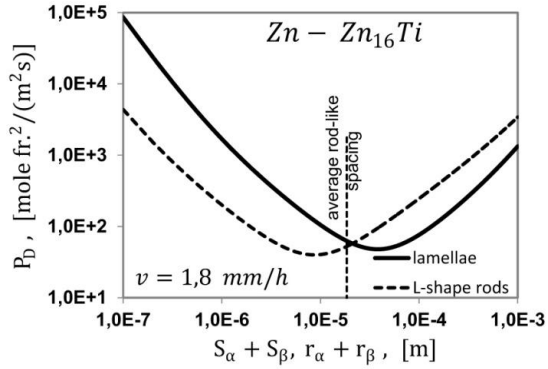

Fig. 10a. Entropy production for two competitive structures: L-shape rod-like and lamellar structures; rates range: $0 < v < v_1$

Average rod-like spacing, Fig. 10a., is the result of calculation of the mean value between regular spacing, width of the non-coupled phase, and wavelength of the perturbation of the s/l interface of the non-faceted (Zn) – phase. The detailed mode of calculation has already been delivered, [14].

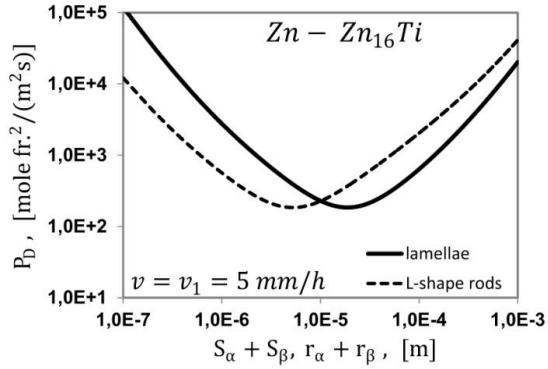

Fig. 10b. Entropy production for two competitive structures: L-shape rod-like and lamellar structures; calculation made for the first threshold growth rate: $v = v_1$; minima are at the same level

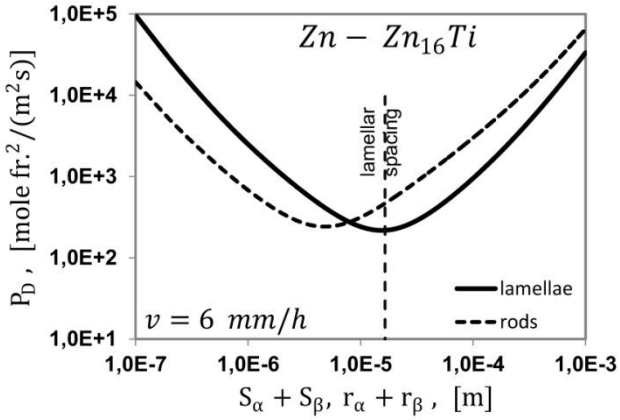

Fig. 10c. Entropy production for two competitive structures: lamellar and rod-like structures; rates range: $v_1^{'} < v < v_2$

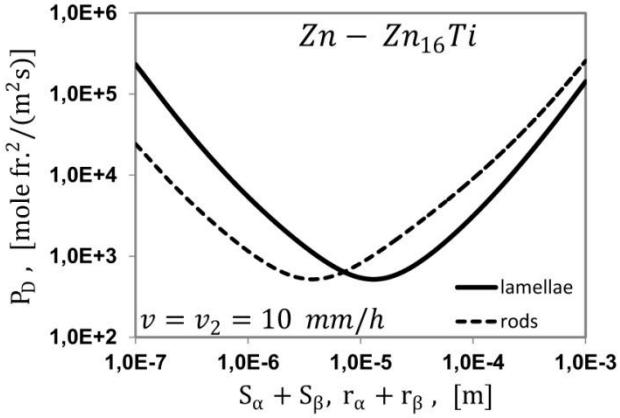

Fig. 10d. Entropy production for two competitive structures: lamellar and rod-like structures; calculation made for the second threshold growth rate: $v = v_2$; minima are at the same level

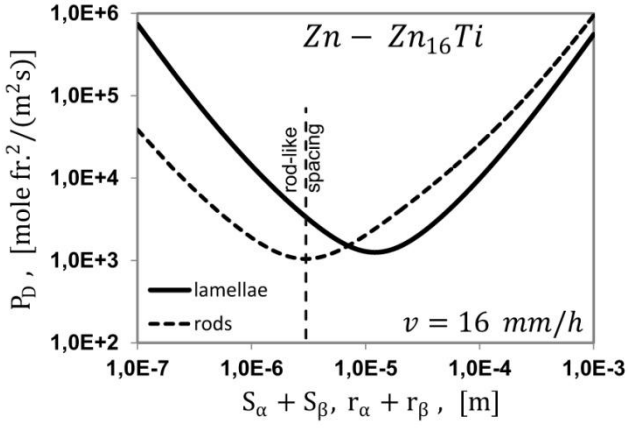

Fig. 10e. Entropy production for two competitive structures: rod-like and lamellar structures; rates range: $v > v_2$

Next, the entropy production was minimized in order to compare its minimal values for all studied ranges of solidification rates. The result of calculation is shown in Fig. 11.

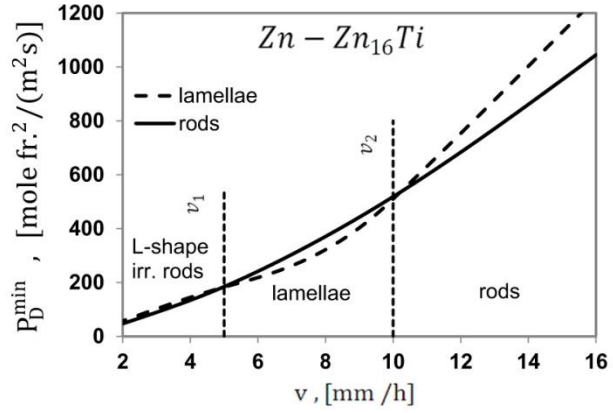

Fig. 11. Comparison of minimal values of the entropy production calculated for both regular rod-like structure formation (forming within two rates ranges) and regular lamellar structure formation

The estimation of the average rod-like spacing for the first rates range: $0 < v < v_1$ required to apply a definition of the mean value of the investigated spacing, [14]:

$$\bar{R} = 0.5R + R_\beta^i + 0.5\lambda_{irr} \tag{11}$$

where $R = 2\left(r_\alpha + r_\beta\right)$, well defined within the areas of the regular structure contained inside the generally irregular structure, R_β^i - radius of the non-coupled rod which manifest significant protrusion over a s/l interface,

$$\lambda_{irr} = 2\pi\left(\Gamma_{(Zn)} / \left(G - m_{(Zn)} G_C\right)\right)^{0.5} \tag{12}$$

is a wavelength of perturbation which appears at the s/l interface of the (Zn) – non-faceted phase, with $\Gamma_{(Zn)}$ - Gibbs-Thomson capillary parameter, G - thermal gradient at the s/l interface, $m_{(Zn)}$ - slope of the liquidus line of the (Zn) – phase, G_C - solute concentration gradient at the s/l interface of the (Zn) - phase.

In the rates range: $v_1 < v < v_1^{'}$ the following transformation occurs:

$$\lambda_{irr} \to R; R_\beta^i \to 0 \text{ and finally } \bar{R} \equiv R \tag{13}$$

It means that irregular structure transforms completely into regular structure. This transformation leads to complete disappearing of branches which were observed below the first threshold growth rate, $v = v_1$.

Additionally, the regular rods transforms into regular lamellae within the rates range, $v_1 < v < v_1^{'}$, Fig. 11.

6. Concluding remarks

According to the developed experiments and simulations the following conclusions can be formulated:

1/ it is possible to control the L - distance between two neighboring stripes, Fig. 2., by imposing a new nominal solute concentration, N_0, as defined in Fig. 1., well visible in Fig. 6.,

2/ it is possible to control the width of the stripes by imposing a proper back-diffusion parameter: $\alpha = \alpha(v)$ with N_0 = const., Fig. 6.,

3/ it is possible to obtain different morphology of the stripes: L-shape rods equipped with branches, regular lamellae, regular rods by applying an adequate growth rate, v, Fig. 11.,

4/ the discussed control of the technological parameters is possible due to the application of:

- the new model for solute redistribution, (2) – (7),
- the new principle of the lower minimum entropy production, (8) – (10), Fig. 10, Fig. 11,
- the model of the anisotropy of the specific surface free energy, Fig. 9, accompanied by the model of the rotation of mechanical equilibrium situated at the tripe point of the solid / liquid (s/l) interface, Fig. 8,
- the new model of the vanishing of branches, (13), accompanied by the model of transformation of the irregular structure into the regular structure, (11) – (13),

5/ it exists few possibilities of the strengthening of the hexagonal (Zn) – single crystal an finally possibilities of the obtaining some new mechanical properties by the creation of:

- an optimal morphology of the Zn16-Ti intermetallic compound within the stripes, Fig. 3, Fig. 11,
- an optimal width of the stripes, Fig. 6,
- an optimal distance between the stripes, Fig. 6.

Acknowledgements

The financial support from the Polish Ministry of Science and Higher Education (MNiSW) under contract N N 508 480038 is gratefully acknowledged.

References

[1] R. Elliott, *Eutectic Solidification*, International Metals Reviews, 219, (1977), 161-186.

[2] H.A. Steen, A. Hellawell, *The Growth of Eutectic Silicon – Contributions to Undercooling*, Acta Metallurgica, 23, (1975), 529-536.

[3] W. Wołczyński, *Lamella / Rod Transformation as described by the Criterion of Minimum Entropy Production*, International Journal of Thermodynamics, 13, (2010), 35-42.

[4] K.A. Jackson, J.D. Hunt, *Lamellar and Rod Eutectic Growth*, Transactions of the Metallurgical Society of the AIME, 236, (1966), 1129-1142.

[5] J.L. Murray, in: *Binary Alloy Phase Diagrams*, edited by T. Massalski, edition of ASM International, (1990), 336-339.

[6] W. Wołczyński, *Back-diffusion Phenomenon during the Crystal Growth by the Bridgman Method*, Chapter 2 in: Modelling of Transport Phenomena in Crystal Growth, edited by J.S. Szmyd & K. Suzuki, edition of the WIT Press Southampton – Boston, (2000), 19-59.

[7] H.D. Brody, M.C. Flemings, *Solute Redistribution in Dendritic Solidification*, Transactions of the Metallurgical Society of the AIME, 236, (1966), p. 615-624.

[8] E. Guzik, W. Wołczyński, *Conditions for Unidirectional Solidification of (Mn,Zn)Fe_2O_4 Ferrite*, in: Ferrites - Proceedings of the Sixth International Conference on Ferrites, edited by T. Yamaguchi & M. Abe, edition of the Japan Society of Powder and Powder Metallurgy, Tokyo – Kyoto, (1992), 340-341.

[9] W. Wołczyński, E. Guzik, *Predictions of the Nature of Microsegregation for the Manganese-Zinc Ferrites Mono-crystallization*, in: Ferrites - Proceedings of the Sixth International Conference on Ferrites, edited by T. Yamaguchi & M. Abe, edition of the Japan Society of Powder and Powder Metallurgy, Tokyo – Kyoto, (1992), 337-339.

[10] E. Scheil, *Uber die Eutektische Kristallisation*, Zeitschrift fur Metallkunde, 34, (1942), 70-80.

[11] W. Wołczyński, B. Billia, *Influence of Control and Material Parameters on Regular Eutectic Growth and Inter-lamellar Spacing Selection*, Materials Science Forum, 215/216, (1996), 313-322.

[12] G. Lesoult, M. Turpin, *Etude Theorique sur la Croissance des Eutectiques Lamellaires*, Memoires Scientifiques de la Revue de Metallurgie, 1969, 66, p. 619-631.

[13] P. Glansdorff, I. Prigogine, *Thermodynamic Theory of Structure, Stability and Fluctuations*, Wiley – Interscience a Division of John Wiley & Sons, Ltd. London–New York–Sydney–Toronto, 1971, 306 pages.

[14] W. Wołczyński, *Thermodynamics of Irregular Eutectic Growth*, Materials Science Forum, 215/216, (1996), 303-12.